QUT

QUTePrints
Open-access archive of QUT research literature

COVER SHEET

Strange, Andrew and Chandran, Vinod and Ralston, Jonathon (2005) Coal Seam Thickness Estimation Using GPR and Higher Order Statistics – The Near-Surface Case. In Proceedings Eighth International Symposium on Signal Processing and Its Applications 2, pp. 855-858, Sydney, Australia.

Copyright 2005 IEEE.

COAL SEAM THICKNESS ESTIMATION USING GPR AND HIGHER ORDER STATISTICS – THE NEAR-SURFACE CASE

Andrew D. Strange, Vinod Chandran, Jonathon C. Ralston[*]

Image and Video Research Lab, Queensland University of Technology,
2 George Street, Brisbane, Q 4001, Australia
a.strange@qut.edu.au

[*] CSIRO, Exploration & Mining, 1 Technology Court, Pullenvale, Q 4069, Australia

ABSTRACT

A novel pattern recognition-based approach to detect near-surface interfaces using ground penetrating radar (GPR) has been reported in [1]. The approach was used to successfully detect interfaces within 5 cm of the ground surface. This technique has been adapted for the important task of layer thickness *estimation* in the near-surface range. This is inherently a difficult problem to solve in practice because the radar echo is often dominated by unwanted components such as antenna crosstalk and ring-down, ground reflection effects and clutter. Features derived from the bispectrum and a nearest-neighbour classifier have been utilized for this processing task. It is shown that unlike traditional second order correlation based methods such as matched filtering which can fail in known conditions, layer thickness estimation using this approach can be reliably extended to the near-surface region.

1. INTRODUCTION

Ground penetrating radar (GPR) is a non-invasive technique used to determine information about media beneath the earth's surface. In impulse GPR systems a short pulse (nanoseconds) of electromagnetic energy is transmitted into the ground. A proportion of this energy is reflected back towards the surface at interfaces of media with differing electromagnetic parameters (permittivity, permeability and conductivity). The amplitude and time delay of these reflections are used to determine information about the sub-surface. There are many applications that use GPR for sub-surface imaging such as buried landmine detection, pavement evaluation and forensic investigations [2].

Traditional techniques for sub-surface interface detection and layer thickness estimation using GPR involve matched filtering and layer stripping [3]. This is a straightforward task when the targets are well separated spatially and have significant permittivity/conductivity contrasts. The terminology "near-surface" is herein defined to represent the case when the target interface is too close to the surface for the matched filter to be a reliable layer thickness estimator.

One important application for GPR layer thickness estimation is horizon control sensing in underground coal mining [4]. In [1], GPR was used to detect coal seam interfaces within 5 cm. In this paper, the interface detection task is adapted to estimate coal layer thickness within the near-surface range of 1-6 cm. A pattern-recognition approach has been adopted using features derived from the bispectrum and a nearest-neighbour classifier. The results show that layer thickness estimation can be reliably extended to the near-surface region where traditional techniques often fail.

2. RADAR SIGNAL PROCESSING

Traditionally, the matched filter is used to detect target reflections in 1-D GPR data. The time delay of the detected reflection is then used in conjunction with the electromagnetic wave propagation velocity to estimate layer thickness. This is a trivial task when the layer interfaces are well separated and site conditions allow for flexibility in the choice of GPR antenna configuration. Depending on the application, the GPR antennas can be mounted above the surface (air-coupled) or in direct contact with the ground (ground-coupled). In the near-surface case, the matched filter becomes unreliable in both antenna mounting configurations due to nuisance components characteristic of GPR systems. The three main nuisance components are the crosstalk (direct transmitter to receiver pulse), ground reflection and antenna ring-down. Figure 1 shows a typical GPR setup configuration and the signal propagation paths.

When the antennas are ground-coupled, the near-surface interface reflection is masked by the crosstalk and antenna ring-down. The adverse effects of these components can occasionally be minimised using background subtraction, which is simply a mean trace removal filter. Background subtraction is reasonably
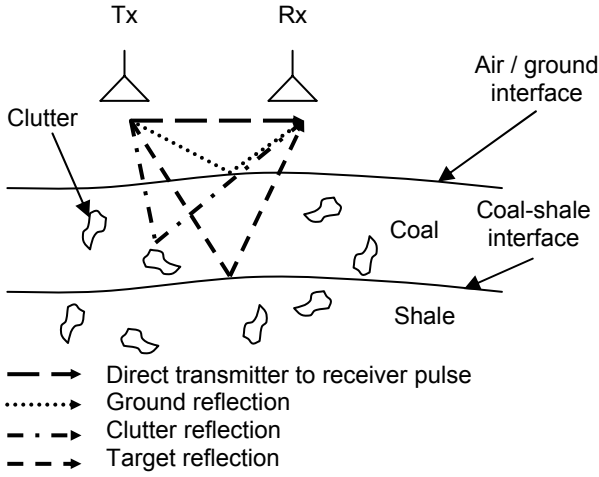
Figure 1. Experimental GPR setup for layer thickness estimation.

Figure 2. Raw GPR trace acquired with ground-coupled antennas. The decaying transient signal is the antenna ring-down.

successful for imaging point reflectors such as a buried landmine or pipe. When estimating layer thickness however, the response from the interface is often removed as it is a plane reflector. In the air-coupled antenna configuration, the crosstalk and ring-down nuisance components are less dominant as they have attenuated before target reflections arrive at the receiver. However the near-surface target reflection is masked by the ground reflection. This is due to the resolution limitation and is dependant upon the wavelength of the transmitted signal. Figure 2 shows a GPR trace acquired with ground-coupled antennas on a coal surface. The large pulse at the start of the trace is the crosstalk and the transient decaying component from 1–3 ns is the antenna ring-down.

For horizon control sensing, the GPR antennas must be in contact with the coal seam as an air-coupled antenna structure would not survive the harsh mining environment [5]. The practical problems of the nuisance components that arise out of the need to use ground-coupled antennas for this task strongly motivate the investigation into alternate processing techniques. To this end we propose the use of pattern recognition techniques for this problem.

3. HIGHER ORDER STATISTICS

The power spectrum is often used as an analysis tool for GPR data [6] because it is simple to apply. However, important information contained in the phase of the radar signal is lost because power spectral representation is a second order measure. This limitation motivates the exploration of higher order spectral processing for this radar processing task as the phase information is retained [7].

The bispectrum $B(f_1, f_2)$ of a discrete-time sequence, $x(n)$, is defined as
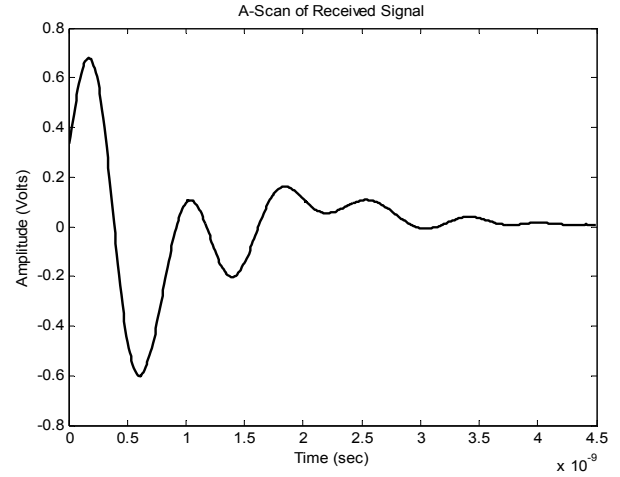
$$B(f_1, f_2) = X(f_1)X(f_2)X^*(f_1 + f_2)$$

where $X(f)$ is the discrete-time Fourier transform of $x(n)$ and * is the complex conjugate operator. Due to symmetry, the bispectrum is defined in the triangular region, $0 \leq f_2 \leq f_1 \leq f_1 + f_2 \leq 1$, provided there is no bispectral aliasing [7].

To obtain a feature that is invariant to translation, amplification, scaling, and DC offset, the bispectrum is integrated radially along lines with slope 'a' as in [7]. The resulting integrated bispectrum has a magnitude and phase component. Typically the phase parameter, which is known for its invariant properties, is used as a feature for classification by a pattern recognition engine. However the implementation of pre-processing algorithms such as DC removal and normalisation extend the invariant properties to the magnitude component. This provides additional feature discrimination compared with the phase parameter feature.

4. EXPERIMENT

A 2-D finite-difference time-domain (FDTD) simulator was implemented to generate the data used for the experiment. The computational space consisted of 250 × 250 cells with grid spacing of 5 mm per cell. Mur's 2nd order absorbing boundary condition (ABC) was implemented to minimise artificial reflections from the boundary [8]. The transmitter and receiver antennas were modeled as small dipoles polarized in the z direction. The ground was modeled as two layers where the top and bottom layers were coal and shale respectively. The electrical parameters (permittivity and conductivity) used in the FDTD algorithm for these layers were measured from real coal and shale samples [1]. In each simulation, the upper layer had a constant

thickness. This layer thickness was changed for each consecutive simulation. The layer thickness range was 0.5-10 cm with 0.5 cm increments.

The pre-processing stage of the feature extraction process included DC offset removal and sum of squares normalisation. The first 128 samples of the 500 samples GPR trace were windowed using a Hamming window. This windowed segment contains the main component of the crosstalk and ringing, and the shape of this segment varies when target interfaces are close to the surface. The final stage before classification is feature standardization [9] to ensure equal weighting between individual feature vector components.

The feature vectors were extracted from the clean synthetic data with known layer thickness. A piecewise polynomial cubic spline was fitted to link the feature vectors obtained from the clean data in increasing layer thickness. The points on the spline from the interpolation are merged with the feature vectors from the synthetic data with known layer thickness to form the full training set. This allows the transition of the thickness estimate towards a continuous variable with sub-millimetre resolution rather than discrete with half centimetre spacing. The thickness estimate is obtained from the single class along the spline contour closest to the test feature vector, which is equivalent to a *k-Nearest-Neighbour* (kNN) classifier with *k=1*. This form of nearest neighbour classification is simplistic yet effective in this application. Figure 3 shows the training feature vectors with known layer thickness at 0.5 cm increments and the cubic spline.

The data used to test the classifier was synthetic with additive Gaussian noise. The noise power was time-varying in nature with a peak of 0.2 mW and zero mean. These noise statistics were measured from the real GPR system adapted for underground coal mining applications described in [1] and [5].

5. RESULTS & DISCUSSION

The cubic spline in Figure 3 shows areas of high concentration of feature values. These regions, between 2.5-3 cm and greater than 6 cm, are susceptible to significant estimation error. The magnitude feature tends to increase as the layer thickness approaches 2.5 cm and then begins to decrease after the 3 cm thickness. This feature change is due to partial constructive and destructive interference between the target reflection and the direct signal component.

Greater layer thicknesses result in the target reflection being delayed along the GPR trace. Hence the early time segment of the trace which is extracted for processing (first 128 samples) has less energy from the target reflection. As the layer thickness increases, the feature vector will converge around the 10 cm point.
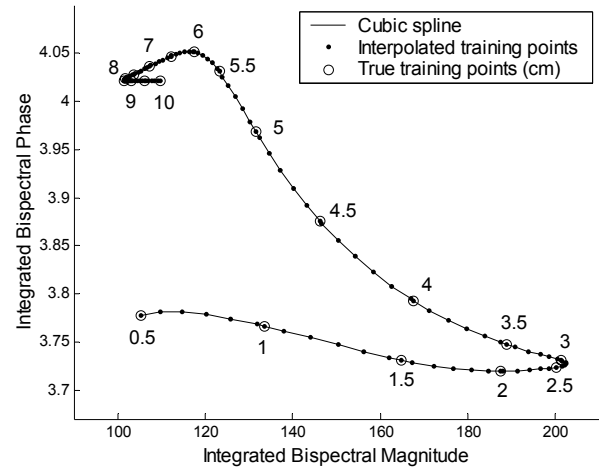

Figure 3. Feature vectors for the training data, interpolated training points and cubic spline.

For the proposed processing technique, this approaches the case when the lower layer is out of range of the GPR system. Hence the current technique is unreliable in this range and traditional techniques such as the matched filter could be the processing tool of choice. The proposed technique could operate in conjunction with the traditional approaches to form a complete layer thickness estimation processing scheme covering the full range from the near-surface to the extent of the GPR range.

The results of the layer thickness estimator are shown in Figure 4 which shows the true layer thickness versus the estimated layer thickness with noisy data over the range 0.5-10 cm. The error bars represent the 99% confidence interval around the estimate mean. As expected from the previous discussion, the region susceptible to estimate errors is the 2.5-3 cm range and above 6.5 cm.
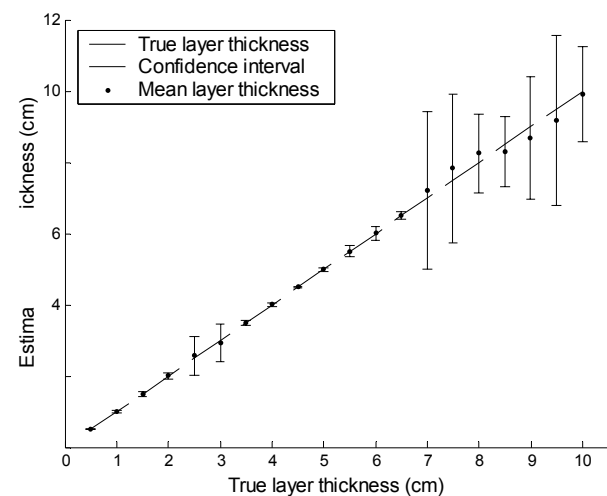
Figure 4. Layer thickness estimator results. The true layer thickness is shown on the *x*-axis whereas the estimated layer thickness is shown on the *y*-axis. The 99% confidence interval is also shown by the error bars.
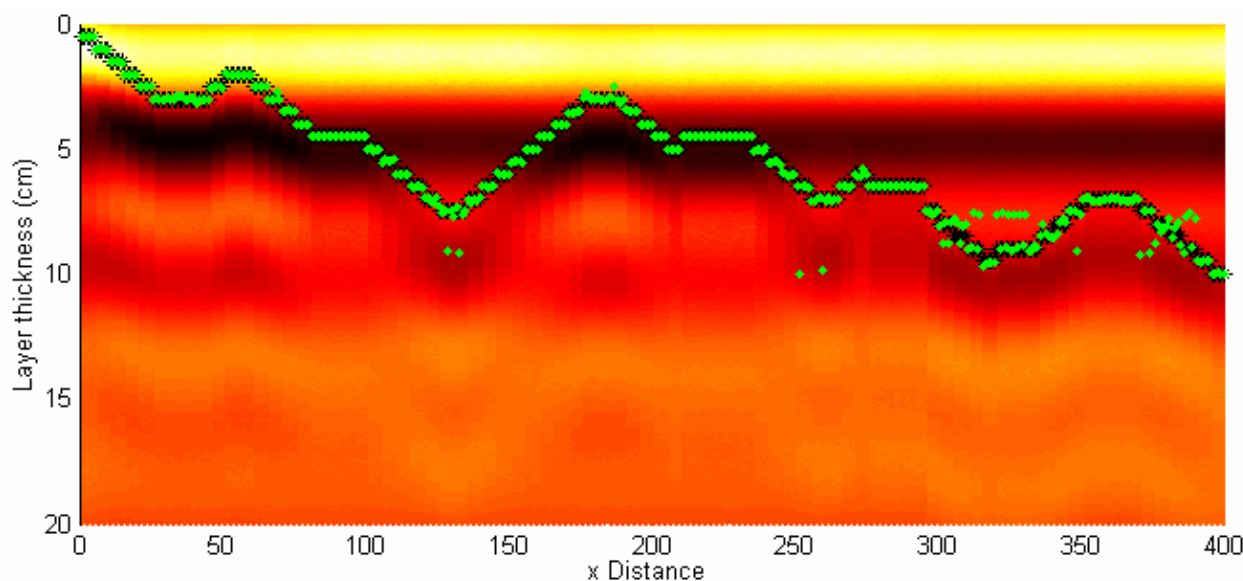
Figure 5. Synthetic GPR data profile of coal-shale interface at varying depth. The true interface depth is shown by the black points, and the estimated depth is shown by the light points.

Figure 5 shows a GPR profile obtained from scanning a coal seam with an underlying shale layer. The synthetic data for this experiment was noisy with the same noise power mentioned above. The coal layer thicknesses shown by the light points are in good agreement with the true layer thickness shown by the black points. The estimator error is clearly visible in outliers when the layer thickness approaches the extent of the near-surface region.

6. CONCLUSION

One application of special interest to the underground coal mining industry is coal layer thickness estimation. One sensor that has shown promise for this task is GPR. However there are certain nuisance components characteristic of GPR systems such as antenna crosstalk and ring-down that make traditional processing techniques such as the matched filter unreliable when target interfaces are close to the surface. As a solution to this problem, a novel pattern recognition-based approach using features derived from the bispectrum and a nearest-neighbour classifier have been developed for this radar processing task. It is shown that unlike traditional second order correlation based methods such as matched filtering which can fail in known conditions, layer thickness estimation can be reliably extended to the near-surface region.

7. REFERENCES

[1] A.D. Strange, J.C. Ralston, and V. Chandran, "Near-surface interface detection for coal mining applications using bispectral features and GPR", *Subsurface Sensing Technologies and Applications,* vol. 6, no. 2, April 2005.

[2] L.P. Peters Jr., J.J. Daniels, and J.D. Young. "Ground penetrating radar as a subsurface environmental sensing tool", *Proc. of the IEEE*, vol. 82, December 1994, pp. 1802-1822.

[3] U. Spagnolini and V. Rampa, "Multitarget detection/tracking for monostatic ground penetrating radar: application to pavement profiling", *IEEE Transactions on Geoscience and Remote Sensing*, vol. 37, January 1999, pp. 383-394.

[4] J.C. Ralston, D.W. Hainsworth, D.C. Reid, D.L. Anderson, and R.J. McPhee, "Recent advances in remote coal mining machine sensing, guidance, and teleoperation", *Robotica*, vol. 19, 2001, pp. 513-526.

[5] W. Murray, C. Williams, J.T.A. Pollock, P. Hatherly, and D.W. Hainsworth, "Ground probing radar applications in the coal industry", in *Proceedings of the 6th International Conference on Ground Penetrating Radar (GPR 96)*, 1996, pp. 107-112.

[6] W. Al-Nuaimy, Y. Huang, M. Nakhkash, M.T.C. Fang, V.T. Nguyen, and A. Eriksen, "Automatic detection of buried utilities and solid objects with GPR using neural networks and pattern recognition". *J. Appl. Geophysics*, vol. 43, 2000, pp. 157-165.

[7] V. Chandran, and S.L. Elgar, "Pattern recognition using invariants defined from higher order spectra – one-dimensional inputs", *IEEE Transactions on Signal Processing*, vol. 41, January 1993, pp. 205-212.

[8] G. Mur, "Absorbing boundary conditions for the finite-difference approximation of the time-domain electromagnetic-field equations", *IEEE Transactions on Electromagnetic Compatibility,* vol. EMC-23, no. 4, November, 1981, pp. 377-382.

[9] R.O. Duda, P.E. Hart, and D.G. Stork, *Pattern classification,* 2nd ed., John Wiley & Sons, NY, 2001.